

Prospects for Lunar Satellite Detection of Radio Pulses from Ultrahigh Energy Neutrinos Interacting with the Moon

O. Stål,^{1,2,*} J. E. S. Bergman,¹ B. Thidé,^{1,3} L. K. S. Daldorff,^{1,3} and G. Ingelman²

¹*Swedish Institute of Space Physics, P.O. Box 537, SE-751 21 Uppsala, Sweden*

²*High Energy Physics, Uppsala University, P.O. Box 535, SE-751 21 Uppsala, Sweden*

³*LOIS Space Centre, Växjö University, SE-351 95 Växjö, Sweden*

The Moon provides a huge effective detector volume for ultrahigh energy cosmic neutrinos, which generate coherent radio pulses in the lunar surface layer due to the Askaryan effect. In light of presently considered lunar missions, we propose radio measurements from a Moon-orbiting satellite. First systematic Monte Carlo simulations demonstrate the detectability of Askaryan pulses from neutrinos with energies above 10^{20} eV, *i.e.* near and above the interesting GZK limit, at the very low fluxes predicted in different scenarios.

PACS numbers: 95.55.Vj, 07.87.+v, 95.55.Jz, 98.70.Sa

Ultrahigh energy cosmic rays (UHECR) provide important information on extreme astrophysical and cosmological processes. Above the Greisen-Zatsepin-Kuzmin (GZK) limit $\sim 5 \times 10^{19}$ eV the universe should be opaque over intergalactic scales to protons due to $p\gamma \rightarrow N\pi$ where γ is a 2.7 K cosmic microwave background photon [1]. The subsequent decays $\pi^+ \rightarrow \mu^+\nu_\mu$ and $\mu \rightarrow e\nu_e\nu_\mu$ give an isotropic flux of “GZK neutrinos” [2, 3] which, if detected, should resolve [4] the apparent contradiction implied by recent observations [5, 6] of cosmic rays with energies above the GZK limit.

Weakly interacting ultrahigh energy neutrinos (UHEC ν) propagate unaffected over cosmic distances, so their arrival directions point back to the original sources. Detection of neutrinos with energies well beyond the GZK limit has also been suggested as a method to test cosmology through the Z-burst process [7], in which the highest energy cosmic rays would be produced following resonant interactions $\nu\bar{\nu} \rightarrow Z^0$ of UHEC ν with cosmological relic neutrinos. In addition to these mechanisms, UHECR and UHEC ν could be produced in the decay of super-heavy relic “X” particles originating *e.g.* from topological defects (TD) associated with Grand Unified Theories [8]. Recent neutrino flux limits, in particular that from ANITA-lite [9], constrain these models and allow only a percent-level contribution to the UHECR from Z-bursts.

No UHEC ν has been observed with existing neutrino telescopes. The next generation km³-sized optical detector Ice-Cube [10] is optimized for 10^{12} – 10^{17} eV neutrinos. At even higher energies, it seems more promising to explore the Askaryan effect [11] of Vavilov-Čerenkov (VC) radio pulse emission from a charged particle shower in a dielectric medium. The shower, initiated by the interaction of a high energy particle, produces via secondary scattering in the medium a net charge excess which radiates coherently for wavelengths longer than the shower dimension. Hence, the power radiated in radio scales quadratically with the initial particle energy and not linearly as in the optical region.

The extremely low flux of UHEC ν necessitates a huge effective target. This can be achieved by the detection of Askaryan pulses from neutrinos interacting with the upper layer (regolith) of the Moon, which has been considered for

Earth-based radio measurements [12, 13, 14, 15, 16, 17], and is currently proposed for a lunar satellite mission [18]. Here, we report Monte Carlo (MC) simulation results on Askaryan pulse detectability with instruments on a satellite orbiting the Moon.

The primary neutrino-nucleon cross sections for deep inelastic charged current (CC) and neutral current (NC) interactions are well-known and can be extrapolated to higher energies [19]. Both CC and NC interactions initiate hadronic showers carrying $E_s = yE_\nu$ of the total neutrino energy E_ν , with $\langle y \rangle = 0.2$ at the very highest energies [19]. As discussed below, we only consider hadronic showers at this stage.

The Askaryan radio emissions from showers in different dielectric media have been parametrized [20, 21, 22] and the results for Silica—the main constituent of the lunar regolith—have been validated in accelerator experiments [23, 24]. In the form given by [17], the spectral flux density F in Jansky (10^{-26} W m⁻² Hz⁻¹) of the VC radiation in a frequency band $\Delta\nu$ around ν , and at an angle θ to the shower axis, from a charged particle shower of total energy E_s inside the lunar regolith can be expressed as

$$F(R, \theta, \nu, E_s) = 1.89 \times 10^9 e^{-Z^2} \left(\frac{\sin \theta}{\sin \theta_{VC}} \right)^2 \left(\frac{E_s}{E_0} \right)^2 \times \left(\frac{R_\zeta}{R} \right)^2 \left(\frac{\nu}{\nu_0 [1 + (\nu/\nu_0)^{1.44}]} \right)^2 \frac{\Delta\nu}{100 \text{ MHz}}. \quad (1)$$

Here, $E_0 = 10^{20}$ eV, $Z = (n \cos \theta - 1)/(\Delta\nu_{VC} \sqrt{n^2 - 1})$, $\nu_0 = 2.5$ GHz is the decoherence frequency where the wavelength becomes comparable to the transverse dimension of the shower, $R_\zeta = 1.738 \times 10^6$ m the lunar radius, R the distance from the source point in the regolith to the detector, and $\Delta\nu_{VC} = 0.0302[\nu_0 L(E_0)]/[\nu L(E_s)]$ radians the angular spread around θ_{VC} . The shower length $L(E_s) = 12.7 + 2/3 \log(E_s/E_0)$ in units of radiation length [17]. The detection threshold in eV is

$$E_s^{\text{th}} = 8.55 \times 10^{20} \frac{R}{R_\zeta} \frac{\nu_0}{\nu} \left[1 + \left(\frac{\nu}{\nu_0} \right)^{1.44} \right] \sqrt{\frac{N_\sigma^2 T_{\text{noise}}}{\Delta\nu A_{\text{eff}}}} \quad (2)$$

in terms of an effective antenna collection area A_{eff} , a radio

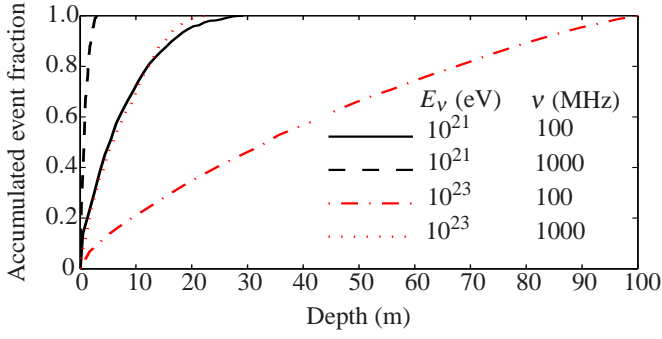


FIG. 1: (color online). Monte Carlo simulation results for the fraction of neutrino events (energy E_v) above a given depth in the Moon, as detected by a tripole antenna (frequency ν) in a Moon-orbiting satellite at 100 km altitude.

system noise temperature T_{noise} , and a minimum detectable radio signal of N_G^2 times the background noise.

Based on properties of lunar soil sample returns [25], we model the regolith down to 100 m depth as a homogeneous dielectric medium with a density of $\rho = 1.7 \times 10^3 \text{ kg/m}^3$ and a radio attenuation length of $l = \lambda / (2\pi n \tan \delta)$ m. To allow for uncertainties in the loss tangent, $\tan \delta$, due to metallic contaminants, we choose the conservative value $\tan \delta = 0.01$ which accounts for the available data. Within uncertainties, this number is also consistent with predictions made for the lunar bedrock layer [25]. Since the attenuation in both materials can be consistently described by a single value, the transition depth becomes unimportant, and our simplified assumption of a deep, homogeneous regolith is justified for our purposes. To estimate the impact of choosing a different depth, below which no neutrino events can be detected, we show in Fig. 1 the accumulated fraction of detected events vs. depth, obtained from simulations as detailed below. The effective depth over which showers are detected is a function of both neutrino energy and observation frequency. The full 100 m depth only contributes for the lowest frequencies and highest neutrino energies. Thus, the curve for $\nu = 100 \text{ MHz}$, $E_v = 10^{23} \text{ eV}$ illustrates the maximum uncertainty.

For the calculation of the emission geometry we use $\theta_{\text{VC}} = 55^\circ$, corresponding to a constant regolith dielectric permittivity $\epsilon = 3$ for the full radio frequency interval considered [25]. The total internal reflection angle θ_{TIR} at the Moon-vacuum interface is complementary to the VC angle. Thus, for a narrow VC cone only emissions from neutrinos which are upward-going with respect to the local surface will escape the Moon. For lower frequencies, when the cone is wider, total internal reflection is not a significant problem since the interface transmission rises rapidly to its maximum value just a few degrees off θ_{TIR} . Rays covering the Δ_{VC} cone are propagated using geometrical optics, taking into account the effects of attenuation, refraction in the (locally flat) Moon-vacuum interface and internal reflection.

In order to estimate the optimum sensitivity in some generality, we use two different approaches to define the radio

sensor equipment. In the first case, an isotropic antenna with dipole characteristics is assumed, representing a low-gain measurement of the complete electric field vector. This can be realized, for instance, using a tripole antenna [26]. The antenna length is taken to be $\lambda/2$ at the highest frequency. It will hence be electrically short over the full bandwidth, which ensures nearly single-mode operation. For an isotropic measurement, the noise temperature T_{noise} is dominated at low frequencies by the galactic background for which we use the simple model $T_{\text{gal}} = 1.5 \times 10^6 (10 \text{ MHz}/\nu)^{2.2} \text{ K}$ [27].

For higher frequencies, the predominant noise contribution is from the radio receiver system and the satellite, assumed at a nominal temperature $T_{\text{sys}} = 300 \text{ K}$. In the second case, a perfectly beam-filling antenna array is assumed, *i.e.* the beam solid angle Ω equals the solid angle of the Moon. The corresponding effective antenna area is then given by $A_{\text{eff}}\Omega = \lambda^2$ and the physical size of the antenna array required to achieve this depends on both frequency and altitude. The assumed directivity towards the lunar surface for this case allows us to set $T_{\text{noise}} = T_{\text{sys}} = 300 \text{ K}$.

Unlike terrestrial measurements of RF transients, a lunar satellite experiment suffers no atmospherics [28]. Likewise, anthropogenic noise, known to interfere badly on Earth [13], is favorably low in the lunar environment, in particular on the far side of the Moon [29]. For Gaussian thermal voltage fluctuations, the single channel rate of spurious triggers, exceeding a level V_0 , is given by $\Gamma_1 = 2\Delta\nu \times P(|V| > V_0) = 2\Delta\nu \times \text{erfc}(N_G/\sqrt{2})$. At 100 MHz bandwidth, $N_G^2 = 25$ gives $\Gamma_1 = 115 \text{ s}^{-1}$. Requiring n -fold coincidence of independent measurements in a time window τ , this rate can be reduced to $\Gamma_n = \tau^{n-1} \Gamma_1^n$. In practice, multiple antennas, frequency bands and/or polarizations are used to define the coincidence channels. To avoid technical details in this generic study, we simulate the detection system using an effective description with full rejection of thermal events and the sensitivity of a single channel. A threshold $N_G^2 = 25$ is used, corresponding to a realistic number for each channel in coincidence (cf. [9]).

For an isotropic neutrino flux $\Phi_\nu(E)$ the number of detected events in the energy interval $[E_1, E_2]$, during time Δt , is

$$N_\nu = \Delta t \int_{E_1}^{E_2} \Phi_\nu(E) \alpha(E) dE \quad (3)$$

where the aperture function $\alpha(E)$ describes the total experimental efficiency as a function of energy. Including the neutrino interaction, radio wave propagation effects and the receiver noise, it represents an equivalent detector area and effective solid angle for which 100% of the incident neutrino flux is detected. This complicated aperture is best studied by MC simulations. For zero detected events (signal and background), a model independent limit [28] on a sufficiently smooth neutrino flux function can be deduced by inverting (3) over an energy interval $dE \sim E$ to obtain

$$E\Phi_\nu(E) \leq \frac{s_{\text{up}}}{\alpha(E)\Delta t} \quad (4)$$

with the Poisson factor $s_{\text{up}} = 2.3$ for a limit with 90% CL.

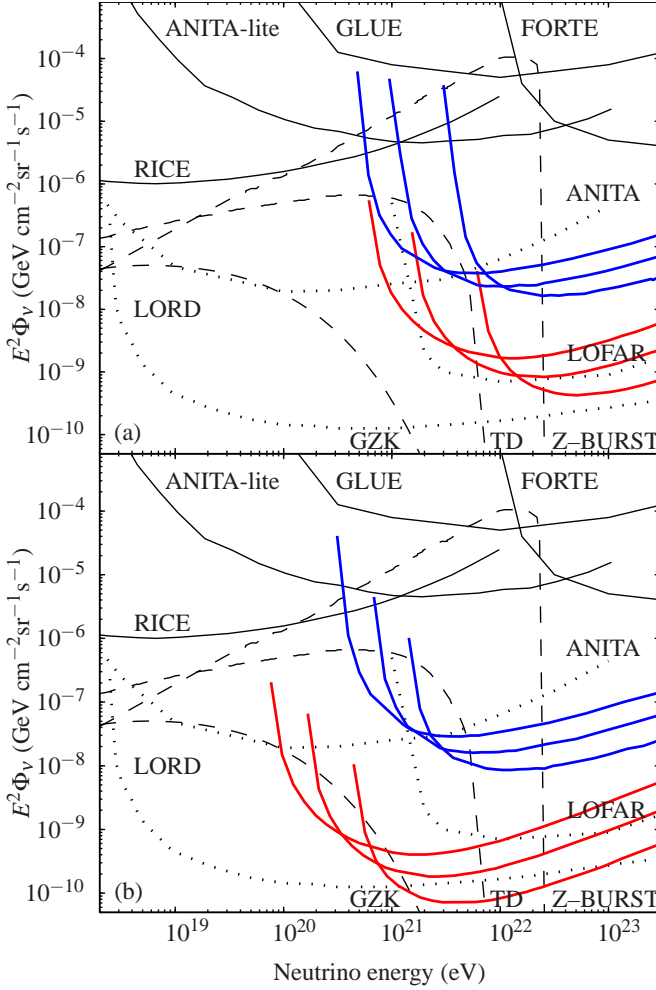


FIG. 2: (color online). E^2 -weighted flux of UHEC ν . Solid (color) curves show the projected detection limits from Eq. (4), based on one year of satellite measurements with (a) a single tripole antenna and (b) a beam-filling antenna for frequencies of 100 MHz (lower set of curves) and 1000 MHz (upper set of curves). Within each set, the curves from top to bottom are for satellite altitudes H of 100, 250 and 1000 km, respectively. Dashed lines show predicted fluxes from the GZK process [3] (consistent with the Waxman-Bahcall bound 5×10^{-8} [33]), Z-bursts and Topological Defects (TD) [30]. Thin solid lines show current flux limits from ANITA-lite [9], RICE [34], GLUE [15] and FORTE [28]. Dotted lines show predicted sensitivities for ANITA [9], LOFAR [17] and LORD [18].

To map out the most favorable conditions for UHEC ν detection we perform MC simulations of the aperture for several values of the center frequency ν and altitude H for a satellite in stationary, circular orbit. The frequency range is limited to 100–1000 MHz, since the narrower VC cone strongly disfavors observations closer to the decoherence frequency ν_0 . Around each center frequency, a symmetric bandwidth of ± 50 MHz is assumed. The altitudes range from 100 to 1000 km. For the beam-filling case, with A_{eff} depending on altitude, also the distance to Earth is considered for comparison. At energies two orders of magnitude above threshold, where the detection starts to become fully efficient, the apertures reach

10^3 – 10^6 km 2 sr for moderate altitudes.

Converting the resultant apertures to limits on the neutrino flux according to Eq. (4), one limit curve is obtained for each parameter pair (ν, H) . Fig. 2 shows the results for an effective observation time of one year, the minimum duration we consider for a lunar satellite mission. The general trend is that lower frequency observations yield more stringent flux limits as a result of the increased angular spread Δ_{VC} of the Askaryan radiation and the longer radio attenuation length in the regolith for lower frequencies. The optimum altitude is less clear. From geometry, the accessible aperture increases with altitude as the visible surface area of the Moon increases, giving stricter limits. However, the threshold energy also increases, which results in the successive shift towards higher energies of the limit curves. As shown in Fig. 2, our flux limits would improve substantially over the existing ones. They would also be competitive, and in some energy regions even better than, the estimated limits that may be obtained by ANITA [9] and LOFAR [17]. Predictions with both higher sensitivity and lower threshold can also be obtained for a lunar satellite experiment, as indicated by the LORD curve [18], assuming that more elaborate antenna setups can be realized.

Since the threshold energy and aperture cannot be varied independently, optimum satellite parameters can only be judged with respect to a specific neutrino flux model. Based on the fluxes from models for GZK, Z-bursts and topological defects, Table I presents integral event rates calculated from Eq. (3). For the Z-burst rates, we conservatively rescale the original flux [30] by a constant factor to conform with the integral bound $E^2\Phi_\nu \leq 1.6 \times 10^{-6}$ GeV cm $^{-2}$ sr $^{-1}$ s $^{-1}$ from ANITA-lite [9]. The rates thus obtained confirm that low frequency observations are most efficient. It is evident that GZK neutrinos cannot be detected in the single tripole case, whereas neutrinos from the other sources can. Here, the lower threshold energy associated with lower altitudes is strongly favorable for the detection of TD neutrinos, while detection of Z-burst neutrinos gains more from the increased aperture at higher altitudes.

In the beam-filling case the antenna gain pattern is adapted to the lunar disc, resulting in higher event rates, but they are even more affected by the choice of observation frequency. The suppressed galactic noise pushes the optimum frequency to its lowest possible value, adding to the effect of an increasing Δ_{VC} . A low frequency beam-filling setup would be able to detect also the GZK neutrinos. For the TD and Z-burst models, the event rates depend weakly on the altitude.

These relatively low rates can be increased through several possible improvements. For CC ν_e events, an additional shower results from the emerging electron, which carries on average 80% of the total neutrino energy. However, for electrons of high energy ($\gtrsim 8 \times 10^{14}$ eV [31]) the cross section to interact with the material is reduced due to the LPM effect [32]. The result is an elongated shower, with a reduced Δ_{VC} [20], and hence smaller detection probability. Still, the electron-initiated showers, from the expected one third of ν_e in the primary neutrino flux, may be further investigated, as

TABLE I: Event rates for satellite observations at frequencies ν and altitudes H based on neutrino fluxes from the GZK process [3], a model for topological defects (TD, with $M_X = 2 \times 10^{13}$ GeV) and Z-bursts ($m_\nu = 0.33$ eV, consistent with cosmological data [30], rescaled by a factor 1.5×10^{-2} to satisfy current flux limits).

Satellite parameters		Integral event rates (yr ⁻¹)		
ν (MHz)	H (km)	GZK	TD	Z-burst
(a) Tripole case				
100	100	4.9×10^{-2}	2.2×10^2	3.3×10^3
100	1000	$< 10^{-5}$	0.0	4.1×10^3
1000	100	6.8×10^{-4}	19	1.5×10^2
1000	1000	$< 10^{-5}$	1.5×10^{-1}	1.9×10^2
(b) Beam-filling case				
100	100	21	6.5×10^3	1.2×10^4
100	1000	6.0	1.5×10^4	7.6×10^4
100	Earth	1.5	1.3×10^4	1.8×10^5
1000	100	2.3×10^{-2}	39	1.9×10^2
1000	1000	1.2×10^{-3}	21	6.2×10^2
1000	Earth	1.5×10^{-4}	7.4	9.9×10^2

may secondary showers from CC ν_τ interactions.

In a more detailed modeling of the lunar composition, also the positive contributions of the bedrock layer should be considered. The higher density means more neutrino interactions per unit volume and showers that develop faster, which gives larger Δ_{VC} and increased detection probability. The effects of surface roughness scattering and possibly diffuse scattering at the rock–regolith interface should then also be considered.

To increase the experimental sensitivity to GZK neutrinos, the threshold energy [Eq. (2)] must be lowered by increasing the effective antenna area, or by decreasing N_σ . This means using more antennas in coincidence and, for the beam-filling case, each with a narrower beam. The sensitivity is limited by what is technically feasible to use on-board a lunar satellite.

In conclusion, we have used MC simulations to demonstrate the prospects for a Moon-orbiting satellite to detect, via the Askaryan effect, ultrahigh energy cosmic neutrinos interacting in the Moon. This method can provide competitive, and in some respects better, conditions compared to Earth-based experiments. For a given lunar mission, the incremental cost for this experiment will not be excessive. For the two specific model cases we consider, neutrino energies above 10^{20} eV can be covered. The flux of GZK neutrinos, which originate from well known Standard Model processes, can be discovered with suitable satellite and antenna parameters. The UHEC ν from proposed exotic sources can be observed even at a much lower flux than predicted, resulting in strict limits to be set or a revolutionary discovery.

We are grateful to V. A. Tsarev and the LORD collaboration for very interesting and useful discussions. Financial support from the Swedish Governmental Agency for Innovation Systems, the Swedish National Space Board and the Swedish

Research Council is gratefully acknowledged. The computer cluster used was funded via an IBM Shared University Research (SUR) grant.

* Electronic address: oscar.stal@tsl.uu.se

- [1] K. Greisen, Phys. Rev. Lett. **16**, 748 (1966); G. T. Zatsepin and V. A. Kuzmin, JETP Lett. **4**, 78 (1966).
- [2] V. S. Berezhinsky and G. T. Zatsepin, Phys. Lett. **28B**, 423 (1969).
- [3] R. Engel, D. Seckel, and T. Stanev, Phys. Rev. D **64**, 093010 (2001); <ftp://ftp.bartol.udel.edu/seckel/ess-gzk/>.
- [4] D. Seckel and T. Stanev, Phys. Rev. Lett. **95**, 141101 (2005).
- [5] M. Takeda et al., Astropart. Phys. **19**, 447 (2003).
- [6] R. U. Abbasi et al., Phys. Rev. Lett. **92** 151101 (2004).
- [7] T. Weiler, Phys. Rev. Lett. **49**, 234 (1982).
- [8] P. Bhattacharjee, C. T. Hill, and D. N. Schramm, Phys. Rev. Lett. **69**, 567 (1992).
- [9] S. W. Barwick et al. (ANITA collaboration), Phys. Rev. Lett. **96**, 171101 (2006).
- [10] J. Ahrens et al. (IceCube collaboration), Astropart. Phys. **20**, 507 (2004).
- [11] G. A. Askaryan, Sov. Phys. JETP **14**, 441 (1962); G. A. Askaryan, Sov. Phys. JETP **21**, 658 (1965).
- [12] R. D. Dagkesamanskii and I. M. Zheleznykh, JETP Lett. **50**, 233 (1989).
- [13] T. H. Hankins, R. D. Ekers, and J. D. O’Sullivan, Mon. Not. R. Astron. Soc. **283**, 1027 (1996).
- [14] J. Alvarez-Muniz and E. Zas, AIP Conf. Proc. **579**, 128 (2001).
- [15] P. W. Gorham et al. (GLUE collaboration), Phys. Rev. Lett. **93**, 041101 (2004).
- [16] A. R. Beresnyak et al., Astron. Rep. **49**, 127 (2005).
- [17] O. Scholten et al., Astropart. Phys. **26**, 219 (2006).
- [18] G. A. Gusev et al. (LORD collaboration), Cosmic Research **44**, 19 (2006).
- [19] R. Gandhi et al., Astropart. Phys. **5**, 81 (1996).
- [20] J. Alvarez-Muniz and E. Zas, Phys. Lett. B **411**, 218 (1997).
- [21] E. Zas, F. Halzen, and T. Stanev, Phys. Rev. D **45**, 362 (1992).
- [22] J. Alvarez-Muniz et al., Phys. Rev. D **68**, 043001 (2003).
- [23] P. W. Gorham et al., Phys. Rev. E **62**, 8590 (2000).
- [24] D. Saltzberg et al., Phys. Rev. Lett. **86**, 2802 (2001).
- [25] G. R. Olhoeft and D. W. Strangway, Earth and Plan. Sci. Lett. **24**, 394 (1975).
- [26] R. T. Compton Jr., IEEE Trans. Ant. and Prop. **29**, 944 (1981); T. Carozzi, R. Karlsson, and J. Bergman, Phys. Rev. E **61**, 2024 (2000).
- [27] F. G. Stremler, *Introduction to Communication Systems* (Addison-Wesley, Reading, MA, 1990), 3rd ed.
- [28] N. G. Lehtinen et al., Phys. Rev. D **69**, 013008 (2004).
- [29] J. K. Alexander et al., Astron. and Astrophys. **40**, 365 (1975).
- [30] D. V. Semikoz and G. Sigl, J. Cosmol. and Astropart. Phys. **04** (2004) 003.
- [31] J. Alvarez-Muniz et al., Phys. Rev. D **74**, 023007 (2006).
- [32] L. D. Landau, J. Phys. U.S.S.R. **8**, 201 (1944); L. D. Landau and I. Pomeranchuk, Dokl. Akad. Nauk S.S.S.R **92**, 735 (1953); A. B. Migdal, Phys. Rev. **103**, 1811 (1956).
- [33] E. Waxman and J. N. Bahcall, Phys. Rev. D **59**, 023002 (1998).
- [34] I. Kravchenko et al. (RICE collaboration), Phys. Rev. D **73**, 082002 (2006).